CHEMISTRY & SUSTAINABILITY

CHEMSUSCHEM

ENERGY & MATERIALS


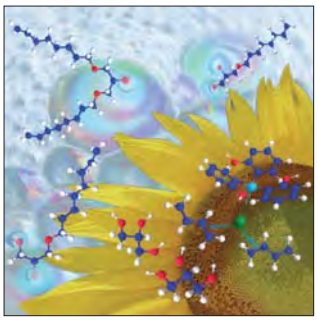
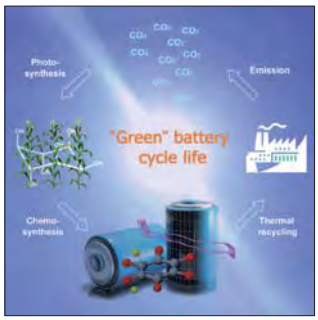

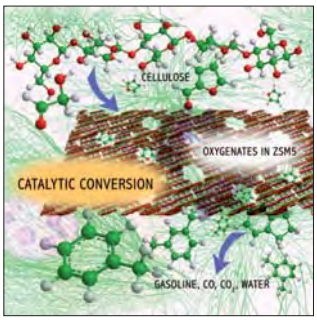

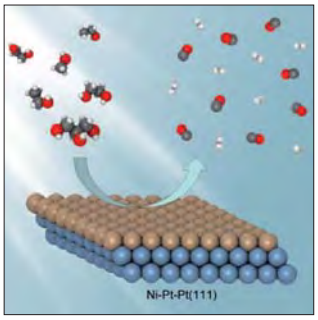

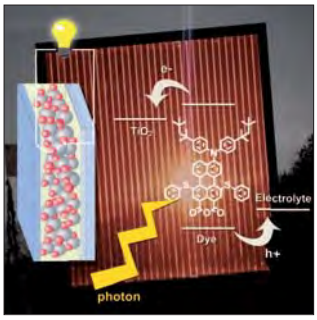

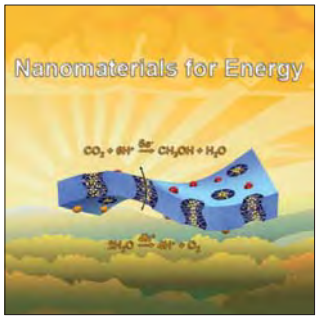

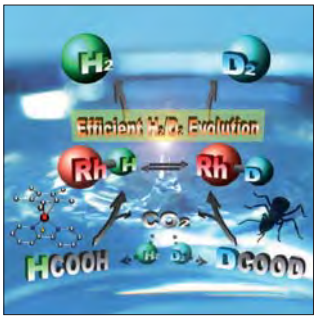

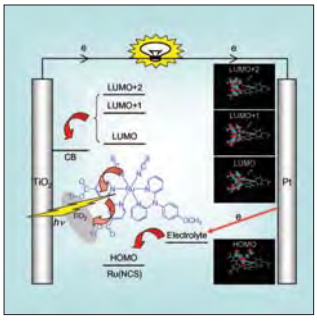

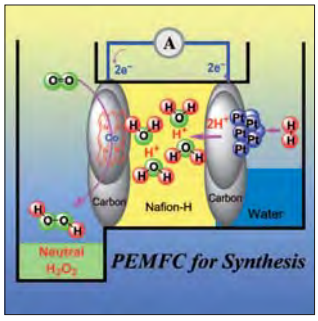

Reprint

ChemPubSoc Europe

WILEY-VCH

Supported by ACES

CHEMISTRY & SUSTAINABILITY
CHEMSUSCHEM
ENERGY & MATERIALS

Table of Contents

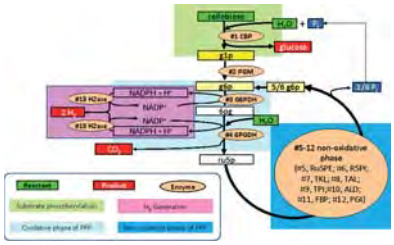

Cocktail reception: Biohydrogen is produced in high yield from cellulosic materials and water in a one-pot process catalyzed by up to 14 enzymes and one coenzyme. This assembly of enzymes results in non-natural catabolic pathways. These spontaneous reactions are conducted under modest reaction conditions (32 °C and atmospheric pressure).

WILEY-VCH

DOI: 10.1002/cssc.200900017

Spontaneous High-Yield Production of Hydrogen from Cellulosic Materials and Water Catalyzed by Enzyme Cocktails

Xinhao Ye,[a] Yiran Wang,[a] Robert C. Hopkins,[b] Michael W. W. Adams,[b] Barbara R. Evans,[c] Jonathan R. Mielenz,[c] and Y.-H. Percival Zhang*[a]

Carbon-neutral hydrogen gas is a future energy carrier, especially for the transportation sector.[1–3] Although hydrogen gas can be produced from a number of hydrogen-containing compounds, such as natural gas and water, low-cost hydrogen production from renewable energy sources is in high demand. The production of biohydrogen from less costly and abundant lignocellulosic biomass under modest reaction conditions may be a cost-effective shortcut because it provides a solution to global-scale solar energy collection and storage and has nearly zero net carbon emissions.[4,5]

Numerous carbohydrate-to-hydrogen conversion approaches have been investigated, involving chemical catalysis, biocatalysis, and combinations of both. Chemical catalysis includes gasification,[6] pyrolysis,[7] ultrafast volatilization,[8] and aqueous-phase reforming.[9] Most biocatalyzed hydrogen is produced through anaerobic dark fermentation with a theoretical maximum yield of four H_2 molecules per glucose, along with two acetate ions.[10] Recently, a bioelectrochemically assisted microbial electrolysis cell was used to convert acetate into hydrogen with help of low-voltage electricity for the high-yield production of hydrogen.[11] A theoretical 10 molecules of H_2 per glucose could be achieved by a combination of biocatalysis and catalysis involving cellulose hydrolysis and glucose-ethanol fermentation,[12,13] followed by ethanol reforming or partial oxidation reforming.[14,15] However, all of these methods still suffer from much lower hydrogen yields than the theoretical maximum yield of 12 molecules of H_2 per glucose.

The feasibility of producing high-yield hydrogen from starch in one reactor has been demonstrated by using an enzyme cocktail containing 13 enzymes.[16] However, only approximately half of a glucose equivalent of soluble starch, a branched polysaccharide, can be converted into glucose-1-phosphate mediated by starch phosphorylase for hydrogen production. The previously reported yield of hydrogen was only 5.19 moles of hydrogen per glucose equivalent of starch consumed, largely due to incomplete reaction.[16] Non-efficient conversion of starch and its limited supplies economically prohibit large-scale hydrogen production through this new approach.

Cellulose, a linear polymer of anhydroglucose, is the most abundant renewable polysaccharide.[13,17,18] Cellobiose is a dominant product of primary enzymatic cellulose hydrolysis,[12] and cellodextrins are prepared in high yields from cellulose or biomass by using mixed acid hydrolysis.[19]

Our goal was to produce hydrogen in high yield from cellulosic materials and water. To fulfill this task, a new synthetic enzymatic pathway was designed (Figure 1). The pathway contains five sub-modules: 1) conversion of cellobiose into glucose-1-phosphate (g1p) catalyzed by cellobiose phosphorylase, 2) generation of glucose-6-phosphate (g6p) from g1p catalyzed by phosphoglucomutase, 3) production of NADPH catalyzed by two dehydrogenases of the oxidative phase of the pentose phosphate pathway (PPP), 4) regeneration of g6p from ribulose-5-phosphate catalyzed by the eight enzymes of the non-oxidative phase of PPP, and 5) generation of hydrogen from NADPH catalyzed by hydrogenase. The overall cellobiose-to-hydrogen reaction can be summarized as shown in Equation (1).

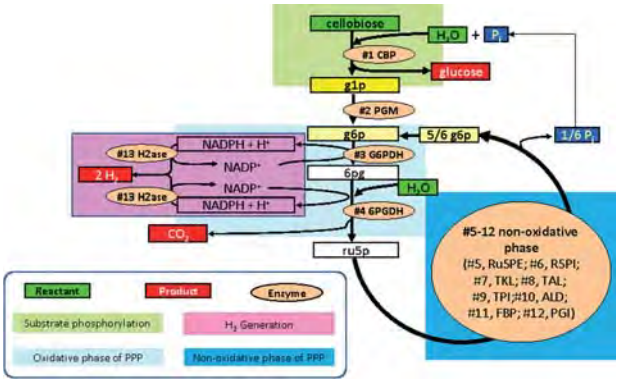

Figure 1. Hydrogen production from cellodextrin and water by a synthetic enzymatic pathway. Enzymes: 1) CBP = cellobiose phosphorylase; 1.1) CDP = cellodextrin phosphorylase; 2) PGM = phosphoglucomutase; 3) G6PDH = glucose-6-phosphate dehydrogenase; 4) 6PGDH = 6-phosphogluconate dehydrogenase; 5) R5PI = phosphoribose isomerase; 6) Ru5PE = ribulose 5-phosphate epimerase; 7) TKL = transketolase; 8) TAL = transaldolase; 9) TPI = triose phosphate isomerase; 10) ALD = aldolase; 11) FBP = fructose-1,6-bisphosphatase; 12) PGI = phosphoglucose isomerase; and 13) H2ase = hydrogenase. Metabolites and chemicals: g1p = glucose-1-phosphate; g6p = glucose-6-phosphate; 6pg = 6-phosphogluconate; ru5p = ribulose-5-phosphate; x5p = xylulose-5-phosphate; r5p = ribose-5-phosphate; s7p = sedoheptulose-7-phosphate; g3p = glyceraldehyde-3-phosphate; e4p = erythrose-4-phosphate; dhap = dihydroxacetone phosphate; fdp = fructose-1,6-diphosphate; f6p = fructose-6-phosphate; and P_i = inorganic phosphate.

[a] X. Ye, Dr. Y. Wang, Prof. Y.-H. P. Zhang
Biological Systems Engineering Department
Virginia Polytechnic Institute and State University
Blacksburg, VA 24061 (USA)
Fax: (+01) 540-231-3199
E-mail: ypzhang@vt.edu

[b] R. C. Hopkins, Prof. M. W. W. Adams
Department of Biochemistry and Molecular Biology
University of Georgia, Athens, GA 30602 (USA)

[c] Dr. B. R. Evans, Dr. J. R. Mielenz
Chemical Sciences Division, Oak Ridge National Laboratory
Oak Ridge, TN 37831 (USA)

Supporting Information for this article is available on the WWW under http://dx.doi.org/10.1002/cssc.200900017.

$$C_{12}H_{22}O_{11(aq)} + 7\,H_2O_{(l)} \rightarrow C_6H_{12}O_{6(aq)} + 12\,H_{2(g)} + 6\,CO_{2(g)} \quad (1)$$

Figure 2 shows the profile of H_2 and CO_2 production from a 2 mM aqueous solution of cellobiose supplemented with $NADP^+$ and phosphate and catalyzed by 13 enzymes. CO_2 was

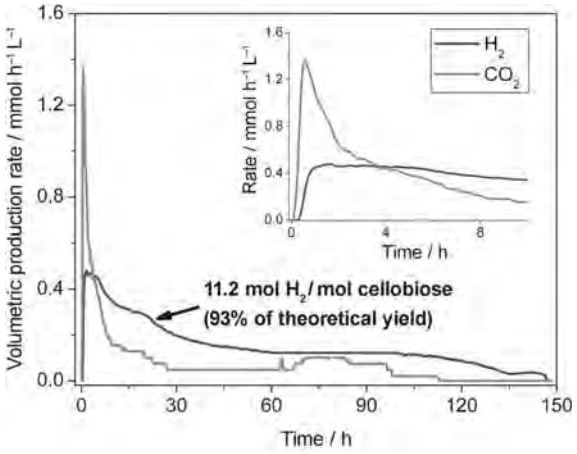

Figure 2. Profile of hydrogen and carbon dioxide production from cellobiose and water.

produced before hydrogen (Figure 2, inset), in good agreement with the reaction mechanism in which enzyme 4 produces CO_2 and NADPH, but enzyme 13 (hydrogenase) produced hydrogen only when the NADPH concentration was sufficiently high.[20] The maximal hydrogen production rate was 0.48 mmol h^{-1} L^{-1} at 1.64 h. After 150 h, H_2 and CO_2 were not detectable in the constantly flushing carrier gas N_2. The overall yields of H_2 and CO_2 were 11.2 mol H_2 and 5.64 mol CO_2 per mole of anhydroglucose unit of cellobiose, corresponding to 93.1% and 94% of the theoretical yields, respectively. The hydrogen yield was comparable to that reported previously (11.6 mol H_2 per mol glucose-6-phosphate).[21] The slightly less than theoretical value was readily explained by accumulated equilibrium intermediates (e.g., g1p, NADPH) in a batch reaction.

Thermodynamic analysis clearly suggested that this cellobiose-to-hydrogen reaction was spontaneous but endothermic (see Supporting Information). To our limited knowledge, this reaction was the first chemical reaction that can absorb ambient-temperature heat and convert it into chemical energy that we can utilize, that is, the output/input (chemical energy) ratio is greater than 1. This reaction was spontaneous ($\Delta G < 0$) when the reaction temperature was higher than 0 °C (Supporting Information), because both gaseous products were released from the aqueous solution under the modest conditions of less than 100 °C and about 1 atm, accompanied with an entropy gain ($\Delta S \gg 0$). Although spontaneous endothermic (entropy-driven) chemical reactions are rare, several examples are reported, such as $N_2O_{5(s)} \rightarrow 2\,NO_{2(g)} + 1/2\,O_{2(g)}$.

Removal of the gaseous products from the aqueous phase at low temperature and pressure decreases product inhibition, simplifies product separation, and promotes the nearly complete overall reaction. However, only one anhydroglucose (C6 unit) of cellobiose (C12) can be used to produce hydrogen so far. The remaining glucose (C6) may be phosphorylized to glucose-6-phosphate by hexokinase at the cost of one ATP per glucose.[21] Unfortunately, utilization of hexokinase and ATP could be economically prohibitive because of 1) costly ATP regeneration system, 2) accumulation of phosphate, an inhibitor of several enzymes (e.g., FBP),[22] 3) precipitation of Mg^{2+} due to high phosphate levels,[22] as Mg^{2+} is a key co-factor of several enzymes, and 4) a pH shift.

To efficiently utilize the glucose equivalents in cellulosic materials, we investigated the production of more g1p from longer-chain cellulosic fragments catalyzed by cellodextrin and cellobiose phosphorylases [Eq. (2)] (*n* corresponds to the degree of polymerization of water-soluble cellodextrins and ranges from 3 to 6).[23,24]

$$G_{n(aq)} + (n-1)\,H_2O_{(l)} + (n-1)\,P_i \rightarrow C_6H_{12}O_{6(aq)} + (n-1)\,g1p \quad (2)$$

With supplement of cellodextrin phosphorylase, the new pathway has a potential to produce more hydrogen (e.g., 12 $(n-1)/n$) per glucose equivalent of longer cellodextrins [Eq. (3)].

$$G_{n(aq)} + 7(n-1)\,H_2O_{(l)} \rightarrow C_6H_{12}O_{6(aq)} + 12(n-1)\,H_{2(g)} + 6(n-1)\,CO_{2(g)} \quad (3)$$

To accelerate hydrogen production rates, we increased the hydrogenase loading and substrate concentration because the metabolic mass flux model suggested that the previous hydrogenase loading limited the overall reaction rates, and that the higher substrate concentrate would lead to the higher reaction rates (Supporting Information). Figure 3 presents the profiles of hydrogen and carbon dioxide production from 2 mM cellopentaose and water. The maximal hydrogen production rate was 3.92 mmol h^{-1} L^{-1}, 8.2-fold higher than that from cellobiose (Figure 2). The overall yields of H_2 and CO_2 were 67.7% and

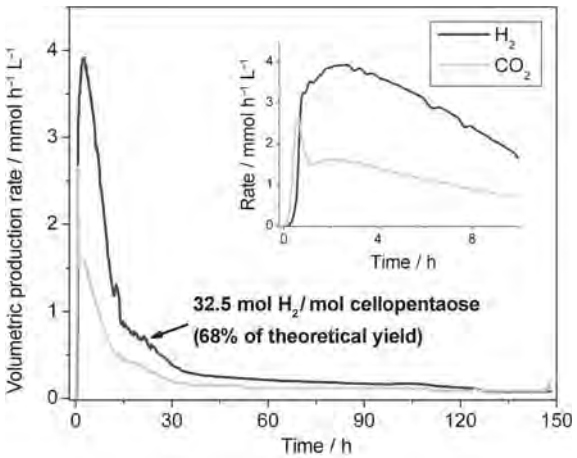

Figure 3. Profile of hydrogen and carbon dioxide production from cellopentaose and water.

70.0% of their theoretical yields, respectively, due to the incomplete reaction at $t = 150$ h (Figure 3).

Two major obstacles must be overcome for future applications, such as the high costs of enzymes and slow reaction rates. The costs associated with the enzymes can be decreased by use of (hyper)thermostable enzymes,[16,21] enzyme immobilization,[25,26] simple enzyme purification,[27,28] and large-scale production of recombinant protein, for example. The long-term stability of immobilized thermostable enzymes has been demonstrated industrially. For example, 1 kg of immobilized glucose isomerase can convert at least 1 500 000 kg of glucose into fructose for several months at around 60 °C before it is deactivated and must be replaced.[5,29] It is anticipated that the rate of biohydrogen production can be accelerated by several orders of magnitude by using a combination of technologies, such as (hyper)thermophilic enzyme replacement, elevated reaction temperatures, optimization of key enzyme ratios, higher substrate concentration, higher enzyme loading, and even metabolite channeling.[5,30,31] For instance, the power densities of microbial fuels cells have been enhanced by approximately 1 000 000-fold during the past decade.[32] In this study, we have increased the hydrogen production rate by 8.2-fold as compared to our previous results on starch[16] by increasing the rate-limiting hydrogenase concentration, increasing the substrate concentration, and by elevating the reaction temperature slightly from 30 to 32 °C. An overall rate enhancement by about 20-fold has been implemented in the past two years (Table 1).

Table 1. Summary of enzymatic hydrogen production rates and yields.

Substrate	Conc. [mM][a]	T [°C]	$V_{max}(H_2)$ [mmol $h^{-1} L^{-1}$]	Yield [%]	Ref.
g6p	2	30	0.21	96.7	[21]
g6p	2	30	0.73[b]	70[c]	[16]
starch	1	30	0.48	43[c]	[16]
cellobiose	2	32	0.48	93.3	this study
cellopentaose	8	32	3.92[d]	67.7[c]	this study

[a] Potential of g6p. [b] The changes as compared to the experiment by Woodward et al.[21] are a reduction in buffer salt concentration and replacement of FBP with a recombinant form. [c] Incomplete batch reaction. [d] The changes compared to the previous results[16] are different combinations of substrate and enzyme, substrate concentration, and concentrations of key enzymes.

In conclusion, the entropy-driven reactions mediated by enzyme cocktails have several unique features: 1) a low-temperature endothermic reaction that absorbs low-temperature thermal energy for producing high-quality chemical energy (hydrogen), 2) a very high demonstrated hydrogen yield (about 11.2 molecules of H_2 per anhydroglucose unit of cellulosic materials) in a batch reaction, and 3) about a 10-fold enhancement in hydrogen production rate compared to that obtained before.[16]

Experimental Section

Enzymes and Their Preparation: All the enzymes are listed in the Supporting Information. Except for the enzymes purchased from Sigma, the recombinant enzymes were prepared as described below. The *cbp*, *cdp*, and *pgm* genes of the thermophilic bacterium *C. thermocellum* ATCC 27405 were amplified by PCR and inserted into the T7-protein expression plasmid pCIG.[27] The recombinant proteins were expressed in *E. coli* BL21 rosetta. The recombinant protein was purified by affinity adsorption on regenerated amorphous cellulose (RAC) followed by intein self-cleavage.[27] The recombinant *E. coli* FBP was expressed and purified as described previously.[22] The *P. furious* hydrogenase I was prepared as described elsewhere and stored at −80 °C.[20] The reaction buffer contained the enzymes (Supporting Information), 0.5 mM thiamine pyrophosphate, 2 mM $NADP^+$, 10 mM $MgCl_2$, and 0.5 mM $MnCl_2$ in a 0.1 M HEPES buffer (pH 7.5). 5 mM 1,4-dithiotreitol (DTT) was added for the cellopentaose experiment.

Experimental Conditions and Data Analysis: The experiments were carried out in a continuous-flow system as described previously,[16] with the modification that 1) ultrapure nitrogen (Air Liquide America Corp., Houston, TX) was used as a carrier gas and 2) the reaction temperature was increased to 32 °C. Hydrogen was measured with a Figaro TGS 822 tin oxide sensor (Figaro Engineering Inc., Osaka, Japan), and carbon dioxide was measured with a LI-COR CO2 Analyzer Model LI-6252 (LI-COR Biosciences Lincoln, NE). Data collection was conducted with the LabView program (National Instruments Corp., Austin, TX), and data analysis was carried out with the MatLab program (Natick, MA).

Acknowledgements

This work was supported by the Air Force Office of Scientific Research (FA9550-08-1-0145), DuPont Young Professor Award, DOE BESC, and ICTAS (all to Y.P.Z.). R.C.H. and M.W.W.A. were supported by a grant from the US DOE (DE-FG02-05ER15710). Previous research at Oak Ridge National Laboratory was funded by the US Department of Energy Office of Energy Efficiency and Renewable Energy (FWP CEEB06). Oak Ridge National Laboratory is managed by UT-Battelle, LLC, for the US Department of Energy under contract DE-AC05-00OR22725.

Keywords: biocatalysis · cellulose · enzyme catalysis · hydrogen

[1] M. Z. Jacobson, W. G. Colella, D. M. Golden, *Science* **2005**, *308*, 1901.
[2] L. Schlapbach, A. Zuttel, *Nature* **2001**, *414*, 353.
[3] A. Cho, *Science* **2004**, *303*, 942.
[4] Y.-H. Zhang, *Public Service Review: European Union, Science & Technology* **2008**, *1*, 126.
[5] Y.-H. Zhang, *Energy Environ. Sci.* **2009**, DOI:10.1039/b818694d.
[6] Y. Matsumura, T. Minowa, B. Potic, S. R. A. Kersten, W. Prins, W. P. M. van Swaaij, B. van de Beld, D. C. Elliott, G. G. Neuenschwander, A. Kruse, M. J. Antal, Jr., *Biomass Bioenergy* **2005**, *29*, 269.
[7] R. M. Navarro, M. A. Pena, J. L. G. Fierro, *Chem. Rev.* **2007**, *107*, 3952.
[8] J. R. Salge, B. J. Dreyer, P. J. Dauenhauer, L. D. Schmidt, *Science* **2006**, *314*, 801.
[9] R. D. Cortright, R. R. Davda, J. A. Dumesic, *Nature* **2002**, *418*, 964.
[10] M. W. W. Adams, E. I. Stiefel, *Science* **1998**, *282*, 1842.
[11] S. Cheng, B. E. Logan, *Proc. Natl. Acad. Sci. USA* **2007**, *104*, 18871.
[12] Y.-H. P. Zhang, L. R. Lynd, *Biotechnol. Bioeng.* **2004**, *88*, 797.
[13] Y.-H. P. Zhang, M. Himmel, J. R. Mielenz, *Biotechnol. Adv.* **2006**, *24*, 452.

[14] G. A. Deluga, J. R. Salge, L. D. Schmidt, X. E. Verykios, *Science* **2004**, *303*, 993.
[15] A. Haryanto, S. Fernando, N. Murali, S. Adhikari, *Energy Fuels* **2005**, *19*, 2098.
[16] Y.-H. P. Zhang, B. R. Evans, J. R. Mielenz, R. C. Hopkins, M. W. W. Adams, *PLoS One* **2007**, *2*, e456.
[17] W. A. Hermann, *Energy* **2006**, *31*, 1685.
[18] Y.-H. P. Zhang, *J. Ind. Microbiol. Biotechnol.* **2008**, *35*, 367.
[19] Y.-H. P. Zhang, L. R. Lynd, *Anal. Biochem.* **2003**, *322*, 225.
[20] K. Ma, Z. H. Zhou, M. W. W. Adams, *FEMS Microbiol. Lett.* **1994**, *122*, 245.
[21] J. Woodward, M. Orr, K. Cordray, E. Greenbaum, *Nature* **2000**, *405*, 1014.
[22] J. L. Donahue, J. L. Bownas, W. G. Niehaus, T. J. Larson, *J. Bacteriol.* **2000**, *182*, 5624.
[23] Y.-H. P. Zhang, L. R. Lynd, *Proc. Natl. Acad. Sci. USA* **2005**, *102*, 7321.
[24] Y.-H. P. Zhang, L. R. Lynd, *Appl. Environ. Microbiol.* **2004**, *70*, 1563.
[25] M. J. Cooney, V. Svoboda, C. Lau, G. Martin, S. D. Minteer, *Energy Environ. Sci.* **2008**, *1*, 320.
[26] M. Moehlenbrock, S. Minteer, *Chem. Soc. Rev.* **2008**, *37*, 1188.
[27] J. Hong, Y. Wang, X. Ye, Y.-H. P. Zhang, *J. Chromatogr. A* **2008**, *1194*, 150.
[28] J. Hong, X. Ye, Y. Wang, Y.-H. P. Zhang, *Anal. Chem. Acta* **2008**, *621*, 193.
[29] S. Bhosale, M. Rao, V. Deshpande, *Microbiol. Rev.* **1996**, *60*, 280.
[30] D. K. Srivastava, S. A. Bernhard, *Science* **1986**, *234*, 1081.
[31] R. J. Conrado, J. D. Varner, M. P. DeLisa, *Curr. Opin. Biotechnol.* **2008**, *19*, 492.
[32] B. E. Logan, J. Regan, *Trends Microbiol.* **2006**, *14*, 512.

Received: January 14, 2009
Published online on February 2, 2009

CHEMISTRY & SUSTAINABILITY
CHEMSUSCHEM
ENERGY & MATERIALS

Supporting Information

Supplementary Online Materials (SOM)

Spontaneous high-yield hydrogen production from cellulosic materials and water catalyzed by enzyme cocktails

Xinhao Ye, Yiran Wang, Robert C. Hopkins, Michael W. W. Adams, Barbara R. Evans, Jonathan R. Mielenz, Y.-H. Percival Zhang

I. Calculation of thermodynamics properties

The overall reaction from cellobiose to hydrogen, carbon dioxide, and glucose is

$$\mathbf{C_{12}H_{22}O_{11}\ (aq) + 7\ H_2O\ (l) \rightarrow C_6H_{12}O_6\ (aq) + 6\ CO_2\ (g) + 12\ H_2\ (g)} \quad \text{(R1)}$$

This reaction can be written as the consequence of two below reactions

$$\mathbf{C_{12}H_{22}O_{11}\ (aq) + H_2O\ (l) \rightarrow 2\ C_6H_{12}O_6\ (aq)} \quad \text{(R2)}$$

$$\mathbf{C_6H_{12}O_6\ (aq) + 6\ H_2O\ (l) \rightarrow 2\ CO_2\ (g) + 12\ H_2\ (g)} \quad \text{(R3)}$$

Thermodynamic parameters of Reaction 2 -- hydrolysis reaction of cellobiose at 298.15 K are $\Delta H_2^o = -2.43\ \text{kJ/mol}$, $\Delta S_2^o = 33.8\ \text{J/mol}$, and $\Delta G_2^o = -12.5\ \text{kJ/mol}$ [1]. Thermodynamic parameters of Reaction 3 were calculated based on the thermo-chemical properties of reactants as well as products. At the standard states, all the data were listed in SOM Table I-1 from the NIST website [2, 3] listed in.

SOM Table I-1. Basic properties of hydrogen, carbon dioxide, water and glucose.

Compound	$\Delta_f H^o$ (kJ/mol)	S^o (J/mol)
$C_6H_{12}O_6$ (l)	-1271.1	209.19
H_2O (l)	-285.83	69.95
H_2 (g)	0	130.68
CO_2 (g)	-393.52	213.79

Thus, the enthalpy and entropy of Reaction 3 are

$$\Delta H_3^o = \sum_{\text{product}} \Delta_f H^o - \sum_{\text{reactant}} \Delta_f H^o = 626.48\ \text{kJ/mol}$$

$$\Delta S_3^o = \sum_{\text{product}} S^o - \sum_{\text{reactant}} S^o = 2221.97\ \text{J/mol}$$

Since $\Delta G = \Delta H - T \cdot \Delta S$, the standard Gibbs free energy (ΔG^o_3) of Reaction 3 was

$$\Delta G_3^o = \Delta H_3^o - T \cdot \Delta S_3^o = -36.38\ \text{kJ/mol}$$

Therefore, thermodynamic properties of Reaction 1 are:

$$\Delta H_1^0 = \Delta H_2^0 + \Delta H_3^0 = 624.05\ \text{kJ/mol}$$

$$\Delta S_1^0 = \Delta S_2^0 + \Delta S_3^0 = 2255.77 \text{ J/mol}$$

$$\Delta G_1^0 = \Delta G_2^0 + \Delta G_3^0 = -48.88 \text{ J/mol}$$

Clearly, Reaction 1 is an endothermic ($\Delta H > 0$) spontaneous ($\Delta G < 0$) entropy-driven ($\Delta S >> 0$) reaction.

We further calculated the properties of Reaction 1 in terms of reaction temperature at 1 atm. Enthalpy change (ΔH) and Gibbs free energy change (ΔG) of Reaction #2 and Reaction #3 can be calculated according to the information [1] and [3], respectively. The heat capacity of glucose was calculated as described elsewhere [4, 5]; the temperature-dependent enthalpy of glucose can be calculated as before [4]; the entropy of glucose can be calculated [6].

SOM Figure I-1 shows the property profile of Reaction 1 in terms of temperature at a fixed pressure (1 atm). Clearly, with an increase in temperature, the Gibbs free energy decreased gradually, suggesting that this spontaneous reaction had more potential for completion. When the reaction temperature is higher than 100°C, water vapor will be mixed with the products, resulting in difficulty in product/reactant separation.

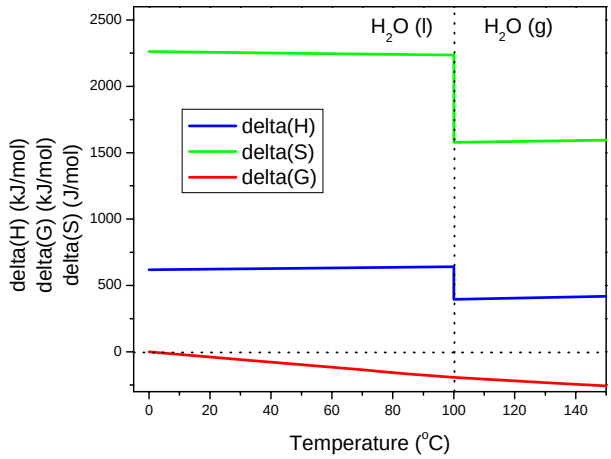

SOM Figure I-1. Profiles of enthalpy, entropy, and Gibbs free energy of Reaction 1 in terms of temperature at 1 atm.

II. Model Simulation of *in vitro* Synthetic Enzymatic Pathway for Novel Hydrogen Production

A mathematical model was developed to simulate hydrogen production from glucose 6-phosate[7], starch[7], and cellobiose. The model consisted of the kinetic equations of the individual reactions and a set of mass balance equations for the different concentrations of each metabolite. The kinetics was based on a modified two-substrate Michaelis-Menten equation except three reactions catalyzed by TKL, TAL, and TPI (SOM Table II-1). Near-equilibrium conditions were assumed for these reactions owing to the respective relatively high Michaelis constant K_m [8]. The mass balances take the following form

$$\frac{dC_i}{dt} = \sum_i v_{ij} r_j$$

where C_i denotes the concentration of metabolite i, and v_{ij} is the stoichiometric coefficient for the metabolite i in reaction j, the rate of which is r_j. Furthermore sensitive analysis is performed based on flux control coefficient (or response coefficient) which was defined as the percentage change in the flux caused by a 1% modulation of the enzyme activity. All in all, the model containing ODEs was solved by Runge-Kutta method and parameters were estimated using derivative-free method, both of which were performed in Matlab 7.0.

A comparison of hydrogen profiles between simulation and experimental data was shown in SOM Figure II-1. The parameters used for computer simulations were listed in SOM table II-1, which were estimated based on the curve-fitting of the CO_2 release rates. The model fit the observed trends reasonably well. However, the largest deviations between measured and predicted value were found after the peak appeared around 200 min, especially for the reactions driven from glucose 6-phosphate. Neither changes in the enzyme loading nor variation in parameter settings leaded to the improvement of the fitting. They might be impaired by the model assumptions that the kinetic parameters kept unchanged if the same enzyme was employed in these three reactions, and that the difference of hydrogen production rate was mainly contributed by the variation of enzyme loading, enzyme activity, and substrates. On the other hand, the remaining deviations between model and measured data also indicated the present limitations in comprehensive modeling bases on mechanistic rate equations [9].

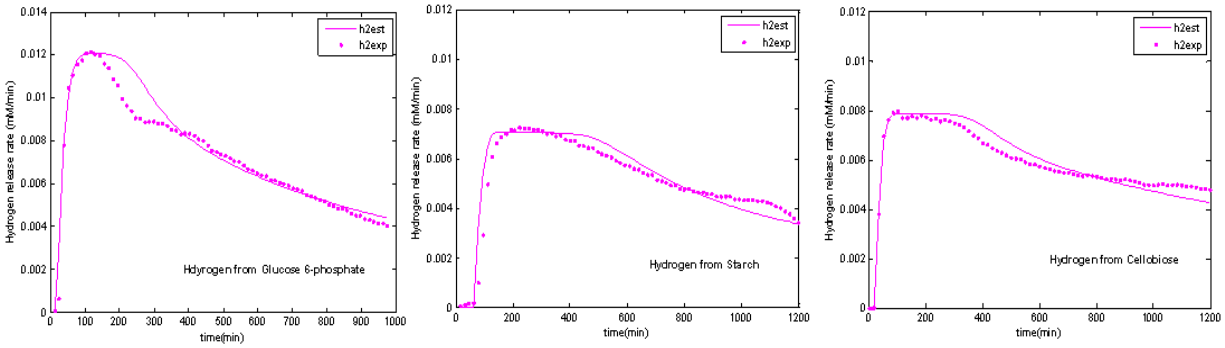

SOM Figure II-1. Comparison between experimental observation (■) and model predictions (lines) for hydrogen evolution rate (mM/min). Left-hand figure illustrates the time curve for G6P reaction, the middle figure is for starch reaction, and the right-hand figure presents the hydrogen evolution from cellobiose.

SOM Table II-1 Kinetic expression and parameters

No	Equation	Parameters	Liter. Data	Estimation		
				G6P	STARCH	CELLOBIOSE
1	$r_1 = r^{GNP} = \frac{k^{GNP}[GNP][G_N][P_i]}{\left[K^{GNP}_{m,Gn}(1+\frac{[P_i]}{K^{GNP}_{I,Pi}})+[G_N]\right]\times\left[K^{GNP}_{m,Gn}+[P_i]\right]}$	$V^{GNP}_{\max}$	-	-	0.10	-
		K^{GNP}_{m,G_n}	0.15[10]	-	0.25	-
		K^{GNP}_{m,P_i}	2.4[10]	-	2.4	-
		K^{GNP}_{i,P_i}	0.14[10]	-	0.12	-
	$r_1 = r^{CBP} = \frac{k^{CBP}[CBP][G_2][P_i]}{\left[K^{CBP}_{m,G_2}(1+\frac{[glc]}{K^{CBP}_{I,glc}})+[G_2]\right]\times\left[K^{CBP}_{m,G_2}+[P_i]\right]}$	$V^{CBP}_{\max}$	-	-	-	0.43
		K^{CBP}_{m,G_2}	7.3[11]	-	-	7.3
		K^{CBP}_{m,P_i}	2.9[11]	-	-	2.9
		$K^{CBP}_{i,glc}$	1.2[11]	-	-	1.2
2	$r_2 = r^{PGM} = \frac{k^{PGM}[PGM]\left([g1p]-[g6p]/K^{PGM}_{eq}\right)}{K^{PGM}_{m,g1p}\left(1+\frac{[g6p]}{K^{PGM}_{I,g6p}}\right)+[g1p]}$	$V^{PGM}_{\max}$	-	-	0.13	0.81
		$K^{PGM}_{m,g1p}$	0.008[12]	-	8.5	0.41
		$K^{PGM}_{m,g6p}$	0.047[12]	-	47	0.50
		K^{PGM}_{eq}	7[12]	-	4	7
3	$r_3 = r^{G6PDH} = \frac{k^{G6PDH}[G6PDH][g6p][NADP]}{\left(K^{G6PDH}_{m,g6p}+[g6p]\right)*\left[K^{G6PDH}_{m,NADP}\left(1+\frac{[NADPH]}{K^{G6PDH}_{I,NADPH}}\right)+[NADP]\right]}$	$V^{G6PDH}_{\max}$	-	0.0287	0.03	0.4
		$K^{G6PDH}_{m,g6p}$	0.034[13]	0.0374	0.0374	0.0374
		$K^{G6PDH}_{m,NADP}$	0.019[14]	0.0223	0.0223	0.0223
		$K^{G6PDH}_{I,NADPH}$	1.7[8]	0.101	0.101	0.101
4	$r_4 = r^{6PGDH} = \frac{k^{6PGDH}[6PGDH][6pg][NADP]}{\left(K^{6PGDH}_{m,6pg}+[6pg]\right)*\left[K^{6PGDH}_{m,NADP}\left(1+\frac{[NADPH]}{K^{6PGDH}_{I,NADPH}}\right)+[NADP]\right]}$	$V^{6PGDH}_{\max}$	-	0.02	0.028	0.13
		$K^{6PGDH}_{m,6pg}$	0.153[15]	0.274	0.2749	0.2749
		$K^{6PGDH}_{m,NADP}$	0.025[15]	0.032	0.032	0.032
		$K^{6PGDH}_{I,NADPH}$	0.055[8]	3.37	3.37	0.082

5	$r_5 = r^{Ru5PE} = \frac{k^{Ru5PE}[Ru5pE] * \left([ru5p] - [x5p]/K_{eq}^{Ru5PE}\right)}{K_{m,ru5p}^{Ru5PE} + [ru5p]}$	$V_{\max}^{Ru5PE}$	-	0.0163	0.03	0.20
		$K_{m,ru5p}^{Ru5PE}$	1.4[16]	0.828	0.828	0.828
		K_{eq}^{Ru5PE}	4[8]	3.46	3.46	3.46
6	$r_6 = r^{R5PI} = \frac{k^{R5PI}[R5PI] * \left([ru5p] - [r5p]/K_{eq}^{R5PI}\right)}{K_{m,ru5p}^{R5PI} + [R5PI]}$	$V_{\max}^{R5PI}$	-	0.0308	0.05	0.10
		$K_{m,ru5p}^{R5PI}$	3.3[17]	3.075	3.075	3.075
		K_{eq}^{R5PI}	1.4[8]	0.25	0.25	0.25
7	$r_7 = r^{TKLa} = k^{TKLa}[TKL] * \left([x5p][r5p] - [s7p][g3p]/K_{eq}^{TKLa}\right)$	$V_{\max}^{TKLa}$	-	0.0392	0.05	0.09
		K_{eq}^{TKLa}	1.2[9]	0.994	0.994	0.994
8	$r_8 = r^{TKLb} = k^{TKLb}[TKL] * \left([x5p][e4p] - [f6p][g3p]/K_{eq}^{TKLb}\right)$	$V_{\max}^{TKLb}$	-	0.0193	0.0193	0.1
		K_{eq}^{TKLb}	10[9]	10.3	10.4	10.3
9	$r_9 = r^{TAL} = k^{TAL}[TAL] * \left([xs7p][g3p] - [f6p][e4p]/K_{eq}^{TAL}\right)$	$V_{\max}^{TAL}$	-	0.0729	0.035	0.08
		K_{eq}^{TAL}	1.05[8]	1.2744	1.27	1.27
10	$r_{10} = r^{TPI} = -\frac{k^{TPI}[TPI] * \left([g3p] - [dhap] * K_{eq}^{TPI}\right)}{K_{m,g3p}^{TPI}(1 + \frac{[dhap]}{K_{m,dhap}^{TPI}}) + [g3p]}$	$V_{\max}^{TPI}$	-	0.0304	0.0304	0.1
		$K_{m,dhap}^{TPI}$	2.11[18]	1.51	1.51	1.51
		$K_{m,g3p}^{TPI}$	3.28[18]	3.53	3.53	3.53
		K_{eq}^{TPI}	0.045[19]	0.0543	0.0543	0.0543
11	$r_{11} = r^{ALD} = \frac{k^{ALD}[ALD] * \left([g3p][dhap] - [fdp]/K_{eq}^{ALD}\right)}{\left(K_{m,g3p}^{ALD}(1 + \frac{[P_i]}{K_{I,Pi}^{ALD}}) + [g3p]\right)\left(K_{m,dhap}^{ALD}(1 + \frac{[P_i]}{K_{I,Pi}^{ALD}}) + [dhap]\right)}$	$V_{\max}^{ALD}$	-	0.047	0.047	0.16
		$K_{m,g3p}^{ALD}$	1[20]	0.790	0.7899	0.790
		$K_{m,dhap}^{ALD}$	2[20]	1.48	1.48	1.48
		K_{I,P_i}^{ALD}	-	6.70	6.70	6.70
		K_{eq}^{TPI}	0.03[21]	0.0241	0.0241	0.0241

12	$r_{12} = r^{FBP} = \frac{k^{FBP}[FBP]*(fdp)}{K_{m,}^{FBP}(1+\frac{[P_i]}{K_{I,Pi}^{FBP}})+[fdp]}$	$V_{\max}^{FBP}$	-	0.032	0.05	0.16
		$K_{m,fdp}^{FBP}$	0.035[22]	0.0434	0.0434	0.0434
		K_{I,P_i}^{FBP}	0.35[22]	0.480	0.480	0.480
13	$r_{13} = r^{PGI} = \frac{k^{PGI}[PGI]*\left([f6p]-\frac{[g6p]}{K_{eq}^{PGI}}\right)}{K_{m,f6p}^{PGI}\left(1+\frac{[g6p]}{K_{m,g6p}^{PGI}}\right)+[f6p]}$	$V_{\max}^{PGI}$	-	0.0329	0.0329	0.16
		$K_{m,f6p}^{PGI}$	0.167[23]	0.159	0.159	0.159
		$K_{m,g6p}^{PGI}$	0.3[24]	0.198	0.198	0.198
		K_{eq}^{PGI}	5[24]	6.27	6.271	6.271
14	$r_{14} = r^{H2ase} = \frac{k^{H2ase}[H2ase]*([NADPH]-[NADP]/K_{eq}^{H2ase})}{K_{m,NADPH}^{H2ase}\left(1+\frac{[NADP]}{K_{I,NADP}^{H2ase}}\right)+[NADPH]}$	K^{H2ase}	-	0.0128	0.0075	0.0084
		$K_{m,NADPH}^{H2ase}$	-	1.74	1.1	1.1
		$K_{I,NADPH}^{H2ase}$	0.063[25]	0.0589	0.0589	0.589
		K_{eq}^{H2ase}	-	15.1	15.1	15.0

One of the goals of our dynamic model was to identify the rate-limiting steps in the synthetic pathway as well as to provide new insights in further enhancement in enzymatic hydrogen production rate and key enzyme properties. Flux control coefficients (FCC) in terms of hydrogen release rate were determined followed by the process simulation. The results were shown in SOM Figure II-2. The highest control was exerted by hydrogenase (#14) as indicated by FCC = 0.95, 0.96, and 0.96 for glucose 6-phosphate reaction, starch reaction, and cellobiose reaction, respectively. Although enzyme loading of hydrogenase was much higher than others (approximately 70 fold), its exhibiting activity was expected to be very low because residual activity of hyper-thermophilic hydrogenase was less than 1 U at 30^{o}C. The low hydrogenase activity not only limited the hydrogen production but also resulted in the accumulation of cofactor NADPH which was a strong inhibitor to other enzymes, such as G6PDH, 6PGDH and hydrogenase itself.

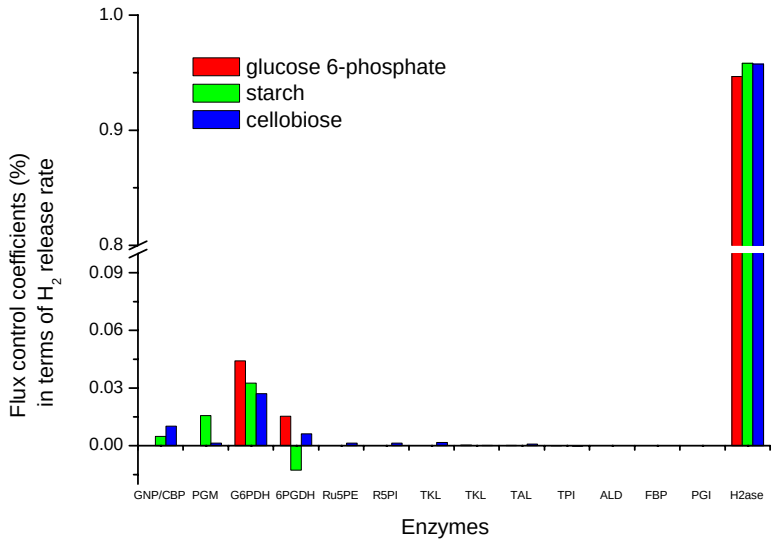

SOM Figure II-2. Flux control coefficients of the enzyme activities on maximum hydrogen production rate.

As a result, the hydrogen production rate can be increased simply by increasing the hydrogenase activity. By *in silico* simulation, 2 fold and 5 fold increases in hydrogenase activity could enhance hydrogen production rates by more than 80% and 150%, respectively.

III. Enzyme information.

SOM Table III-1. The designated number, enzyme catalogue number, full name and abbreviated name of the enzymes as well as their source, preparation, and units used in the experiments.

		Enzyme				Cellobiose (IU/reactor)		Cellopentaose (IU/reactor)	
NO	**EC**	Full name	Abb.	**Source**	**Vendor**	Added*	T-Adj.**	Added*	T-Adj.**
1	2.4.1.20	cellobiose phosphorylase	CBP	*C. thermocellum*	lab	8 [a]	8	4 [a]	4
1.1	2.4.1.49	cellodextrin phosphorylase	CDP	*C. thermocellum*	lab			0.5 [b]	0.5
2	5.4.2.2	phosphoglucomutase	PGM	*C. thermocellum*	lab	10 [c]	10	4 [c]	4
3	1.1.1.49	glucose 6 phosphate dehydrogenase	G6PDH	*S. cerevisiae*	Sigma	5 [d]	8	5 [d]	8
4	1.1.1.44	6-phosphogluconic dehydrogenase	6PGDH	*S. cerevisiae*	Sigma	1 [e]	0.38	1 [e]	0.38
5	5.1.3.1	ribulose 5-phosphate 3-epimerase	Ru5PE	*S. cerevisiae*	Sigma	1 [f]	1.6	1 [f]	1.6
6	5.3.1.6	ribose 5-phosphate isomerase	Ru5PI	*spinach*	Sigma	1 [g]	1	1 [g]	1
7	2.2.1.1	Transketolase	TKL	*E. coli*	Sigma	1 [h]	1.6	1 [h]	1.6
8	2.2.1.2	Transaldolase	TAL	*S. cerevisiae*	Sigma	1 [i]	1.6	1 [i]	1.6
9	5.3.1.1	triose-phosphate isomerase	TPI	*rabbit muscle*	Sigma	4.8 [j]	7.68	4.8 [j]	7.68
10	4.1.2.13	aldolase	ADL	*rabbit muscle*	Sigma	1 [k]	1.6	1 [k]	1.6
11	3.1.3.11	fructose-bisphosphatase	FBPase	*E. coli*	lab	1 [l]	1.6	1 [l]	1.6
12	5.3.1.9	phosphoglucose isomerase	PGI	*S. cerevisiae*	Sigma	1 [m]	1.6	1 [m]	1.6
13	1.12.1.3	*P. furiosus* hydrogenase I	H2ase	*P. furisous*	lab	~100 [n]	3.65	~200 [n]	7.2

* the enzyme activities were determined based on international unit (IU) definition under their optimal or experimental conditions.

** the T-adjusted enzyme activities were estimated based on the rule of thumb for the relationship between the enzyme activity and reaction temperature (doubled enzyme activity per ten degree increase) [14, 26]. The real enzyme activities cannot be measured exactly due to the presence of other factors (enzymes, cofactors, and so on) [27].

[a], the CBP activity was measured by a discontinuous assay coupled with glucose 6-phosphate dehydrogenase from glucose HK kit (Sigma, MO, US). Formation of glucose 6-phosphate from glucose 1-phosphate was measured by monitoring NADPH formation. The initial reaction was conducted at 32^{o}C with 2 mM cellobiose, 4 mM phosphate, 10 mM Mg^{2+}, 0.5 mM Mn^{2+}, 20 μg/ml phosphoglucomutase (~10 U/ml), and 1 mg/ml BSA in 50 mM HEPES buffer, pH7.5, and stopped by heating the samples in boiling water bath for 5 min. Coupled with glucose 6-phosphate dehydrogenase, the formation of NADPH was then determined at the 2nd reaction by measuring the change in absorbance at 340 nm for 15 min. One unit of CBP is defined as the amount of enzyme that generated 1 μmol of NADPH per min.

[b]. the CDP activity was determined similarly with CBP assay, except using 2 mM cellopentaose rather than cellobiose, and pulsing 5 mM DTT. One unit of CDP is defined as the amount of enzyme that generated 1 μmol of NADPH per min under the conditions described.

[c]. the PGM activity was assayed by the discontinuous assay coupled with glucose 6-phosphate dehydrogenase from glucose HK kit (Sigma, MO, US). The initial reaction was performed at 32 ^{o}C with 50 mM HEPES buffer (pH7.5) with 5 mM glucose 1-phosphate, 10 mM Mg^{2+}, 0.5 mM Mn^{2+} and 1 mg/ml BSA. The reaction was stopped by heating the samples in boiling water bath for 5 min. Then the product glucose 6-phosphate was detected by glucose HK kit. One unit of PGM is defined as the amount of enzyme that generated 1 μmol of NADPH per min under the above conditions.

[d]. one unit of G6PDH can oxidize 1.0 μmole of glucose 6-phosphate to 6-phospho-D-gluconate per min in the presence of NADP at pH 7.4 at 25°C.

[e]. one unit of 6PGDH can oxidize 1.0 μmole of 6-phospho-D-gluconate to D-ribulose 5-phosphate and CO_2 per min at pH 7.4 at 37°C in the presence of $NADP^{+}$.

[f]. one unit of Ru5PE can convert 1 μmole of D-ribulose 5-phosphate to xylulose 5-phosphate per min at pH 7.7 at 25°C when coupled with transketolase, α-glycerophosphate dehydrogenase, and triosephosphate isomerase

[g]. one unit of Ru5PI can convert 1.0 μmole of D-ribose 5-phosphate to D-ribulose 5-phosphate per min at pH 7.7 at 30 °C.

[h]. one unit of TKL can produce 1 μmol of glyceraldehyde-3-phosphate from xylulose-5-phosphate per minute at pH 7.7 and 25°C, in the presence of ribose-5-phosphate, thiamine pyrophosphate and Mg^{2+}.

[i]. One unit of TAL can produce 1.0 μmole of D-glyceraldehyde 3-phosphate from D-fructose 6-phosphate per min in the presence of D-erythrose 4-phosphate, at pH 7.7 at 25°C in a coupled system with GDH/TPI and β-NADH.

[j]. One unit of TPI can convert 1.0 μmole D-glyceraldehyde 3-phosphate to dihydroxyacetone phosphate per min at pH 7.6 at 25 °C.

[k]. One unit of ADL can convert 1.0 μmole of fructose 1,6-diphosphate to dihydroxyacetone phosphate and glyceraldehyde 3-phosphate per min at pH 7.4 at 25 °C.

[l]. One unit of FBP can produce 1 μmol of phosphate in 1 min from fructose-1,6-biphosphate as described before [22].

[m]. One unit of PGI can convert 1.0 μmole of D-fructose 6-phosphate to D-glucose 6-phosphate per min at pH 7.4 at 25 °C.

[n]. One unit of hydrogenase I can 1μmole of H_2 per min at 80 °C, as described elsewhere [28].

SOM References

[1] Y. Tewari, R. Goldberg, *J. Biol. Chem.* **1989**, *264*, 3966.
[2] NIST.
[3] M. Chase, in *In J. Phys. Chem. Ref. Data, Monograph 9*, **1998**, pp. 1.
[4] T. Douglas, A. Ball, J. Torgesen, *J. Am. Chem. Soc.* **1951**, *73*, 1360.
[5] D. Ginnings, T. Douglas, A. Ball, *J. Res. Nat. Bureau Standards* **1950**, *45*, 23.
[6] J. Boerio-Goates, *J. Chem. Thermodynamics* **1991**, *23*, 403.
[7] Y.-H. P. Zhang, B. R. Evans, J. R. Mielenz, R. C. Hopkins, M. W. W. Adams, *PLoS One* **2007**, *2*, e456.
[8] S. Vaseghi, A. Baumeister, M. Rizzi, M. Reuss, *Metabolic Engineering* **1999**, *1*, 128.
[9] C. Chassagnole, N. Noisommit-Rizzi, J. W. Schmid, K. Mauch, M. Reuss, *Biotechnology and Bioengineering* **2002**, *79*, 53.
[10] R. MOSI, S. G. WITHERS, *Biochem. J.* **1999**, *338*, 251.
[11] J. K. Alexander, *J. Biol. Chem.* **1986**, *243*, 2899.
[12] O. H. Lowry, J. V. Passonneau, *J. Biol. Chem.* **1969**, *244*, 910.
[13] R. N. Horne, W. B. Anderson, R. C. Nordlie, *Biochemistry* **1970**, *9*, 610.
[14] Y.-H. P. Zhang, L. R. Lynd, *Biotechnol. Bioeng.* **2004**, *88*, 797.
[15] A. R. Rendina, J. D. Hermes, W. W. Cleland, *Biochemistry* **1984**, *23*, 6257.
[16] Bar J, Naumann M, Reuter R, K. G., *Bioseparation* **1996**, *6*, 233.
[17] W. W. Woodruff, 3rd, R. Wolfenden, *J. Biol. Chem.* **1979**, *254*, 5866.
[18] M. M. Greenberg, T. T. T. Yen, J. L. Bobbitt, *European Journal of Biochemistry* **1972**, *24*, 416.
[19] E. A. Noltmann, in *The Enzymes, Vol. 5*, 3rd ed. (Ed.: P. D. Boyer), Academic Press, New York, **1972**, pp. 271.
[20] D. E. Morse, B. L. Horecker, in *Advances in Enzymology and Related Areas of Molecular Biology, Vol. 31* (Ed.: F. F. Nord), Interscience Publishers, New York, **1968**, pp. 125.
[21] G. M. Lehrer, R. Barker, *Biochemistry* **1970**, *9*, 1533.
[22] J. L. Donahue, J. L. Bownas, W. G. Niehaus, T. J. Larson, *J. Bacteriol.* **2000**, *182*, 5624.
[23] M. Marchand, U. Kooystra, R. K. Wierenga, A.-M. Lambeir, J. Van Beeumen, F. R. Opperdoes, P. A. M. Michels, *European Journal of Biochemistry* **1989**, *184*, 455.
[24] M. B. U. T. M. R. Manfred Rizzi, *Biotechnology and Bioengineering* **1997**, *55*, 592.
[25] K. Ma, R. Weiss, M. W. W. Adams, *J. Bacteriol.* **2000**, *182*, 1864.
[26] I. A. Berg, D. Kockelkorn, W. Buckel, G. Fuchs, *Science* **2007**, *318*, 1782.
[27] B. Teusink, J. Passarge, C. A. Reijenga, E. Esgalhado, C. C. van der Weijden, M. Schepper, M. C. Walsh, B. M. Bakker, K. van Dam, H. V. Westerhoff, J. L. Snoep, *Eur. J. Biochem.* **2000**, *267*, 5313.
[28] F. O. Bryant, M. W. Adams, *J. Biol. Chem.* **1989**, *264*, 5070.